Classification of retinopathic injury using image cytometry and vasculature complexity

K. Staniszewski[a§], R. Sepehr[a§], C. M. Sorenson[b], N. Sheibani[c], M. Ranji*[a]
[a]Biophotonics Laboratory, Dept. of Electrical Engineering, University of Wisconsin Milwaukee, 3200 N. Cramer St., Milwaukee, WI USA 53211-3029;
[b]Dept. of Pediatrics, Univ of Wisconsin School of Medicine and Public Health, 600 Highland Avenue, Madison, WI, USA 53792-4673
[c]Dept. of Ophthalmology and Visual Sciences, Univ of Wisconsin School of Medicine and Public Health, 600 Highland Avenue, Madison, WI, 53792-4673

ABSTRACT

Retinopathic injuries are a common symptom of many diseases. However, if detected early, much of the damage caused by these injuries can be prevented, or in some cases reversed. In this study, images of retinas were classified as normal or injured using the vascular cell count, vasculature coverage, and vessel caliber. To model retinal vasculopathies, retinal vasculature from mice with the BCL-2 gene either partially or completely knocked out were compared. The *bcl-2* gene is a critical regulator of apoptosis and angiogenesis, and therefore its absence has a significant impact on the number of vascular cells and vasculature complexity. When the aforementioned features were extracted from the images, classification was performed using a majority vote between a linear classifier, k-nearest-neighbors classification, and a support vector machine. This resulted in a classification accuracy of 81% using the "leave one out" error determination method.

Keywords: Retinopathy, Fluorescence Microscopy, Image Cytometry, Classification, Apoptosis, Angiogenesis

1. INTRODUCTION

Retinopathy is a common symptom of many ocular disorders including, but not limited to, diabetes[1], hypertension[2], and age related macular degeneration[3]. These symptoms may also involve growth of new blood vessels in the retina and leakage of blood from these vessels[4]. As a result, a patient may gradually lose vision and if not treated will result in blindness[5]. Unfortunately, current diagnosis techniques, such as optical coherence tomography, are not sensitive enough to detect early changes in the retinal vasculature prior to significant cellular and vascular damage[6]. Nevertheless, once detected, the damage can be treated to stop, or in rare cases, reverse the pathology incurred[7]. In fact, recent research has shown that earlier diagnosis could lead to a significant reduction in the number of cases of retinopathy[8]. Therefore, it would be beneficial to create a system for detecting these changes in their early stages to prevent further loss of vision. With this end in mind, we have created a software package to determine whether or not a retina has undergone retinopathic injury. This package is capable of analyzing bright field and fluorescent images of the retina and classifies them as healthy or injured in a short period of time, allowing for a possible application in clinical settings. In order to quantify the amount of injury experienced by the retina, the package measures the cell count, vessel coverage, and vessel caliber of high resolution fields of view in the retina, all of which have been shown to correlate with retinopathies[9-12]. The package then uses classification techniques to determine whether or not the retina's vascular integrity has been compromised. Finally, to verify the results of the classification, the leave one out cross-validation method was used, in which one of the data points is withheld from the system during its training phase, and then the point is classified using the newly-trained system.

§ Both authors have contributed equally
* ranji@uwm.edu; Phone: (414) 229 5889; https://pantherfile.uwm.edu/ranji/www/

Imaging, Manipulation, and Analysis of Biomolecules, Cells, and Tissues X, edited by Daniel L. Farkas, Dan V. Nicolau, Robert C. Leif, Proc. of SPIE Vol. 8225, 822526 · © 2012 SPIE · CCC code: 1605-7422/12/$18 · doi: 10.1117/12.908598

2. MATERIALS AND METHODS

2.1 Tissue preparation

To obtain retinas with differing vasculature complexity, mice were compared with either a partial or complete knockout of the BCL-2 gene. The *bcl-2* gene plays an important role in regulating apoptosis and angiogenesis, and its absence is associated with decreased number of vascular cells and vascular density in the retina[13]. Thus, retinas from complete knockout mice have a different cell count and vasculature complexity than their partial knockout counterparts. Verification of the knockout mice was performed by genotyping the litters of mice using PCR of DNA extracted from tail biopsies.

Mice, at 3 or 6 weeks of age, were sacrificed, eyes were removed, and were fixed in 4% paraformaldehyde (10 minutes on ice) for a brief period. The eyes were then fixed in 70% ethanol for at least 24 hours at -20°C. Retinas were then dissected in PBS, washed with PBS three times for 10 minutes each, and were incubated in a blocking buffer for 2 hours. The retinas were then incubated with rabbit anti-PECAM-1 (R&D, Minneapolis, MN) at 4°C overnight. The retinas were again washed with PBS three times, ten minutes each, and incubated with Alexa 594 goat-anti-rabbit for 2 hours at room temperature. Finally, the retinas were washed four times with PBS at 30 minutes each, and mounted on a slide using a mixture of PBS and glycerol. This staining allows for fluorescence imaging of the retinal vasculature using a green excitation and red emission filter pair.

2.2 Imaging

The retinas were imaged using an inverted fluorescence microscope (Nikon Ti-E) at a magnification of 40x. The images were captured using a CCD camera (QImaging EXi Aqua) at a resolution of 1392 x 1040 pixels, leading to a scale of approximately 0.16 um per pixel. The fluorescence filter set used was G-2E/C, which filters the excitation light at 540 nm (25nm bandwidth) and the emission light at 620 nm (60 nm bandwidth), and separates excitation and emission light at 565 nm. This was chosen to agree with the Alexa 594 staining previously mentioned. Each region was then imaged using bright field illumination to determine cell locations and counted 8 fields of view were randomly chosen from each group with these settings.

Once the fluorescence images were acquired, they were thresholded using the histograms of intensity values in the red channel to separate vasculature from background. The histogram of these images shows a bimodal distribution, where the lower intensity mode corresponds to background and the higher intensity mode corresponds to vasculature. With this in mind, the threshold level is determined independently for each image as the minimum value of the histogram (i.e. the least frequent intensity) between these two modes, leading to a binary image which contains the structure of the vasculature.

2.3 Cell detection and count

The location of cells in each image was determined using the following segmentation algorithm. The location of foreground markers (cells) was detected by applying an FIR semi-Laplacian filter to enhance the contrast of the circular objects (using the center and surround method). The background markers were computed by applying watershed detection on the resultant binary mask of the previous stage. Then the gradient of the images is calculated and modified so that its intensity becomes zero in both foreground and background objects. The watershed transform of the modified gradient image is computed and results in a binary mask containing the borders of the objects. Automatic cell segmentation resulted in an accuracy of ~90% compared to manual cell detection and counting.

2.4 Vessel coverage, caliber and length

Since one of the markers of retinopathy is a more dense vasculature, the total vessel coverage was determined for each field of view. This was simply recorded as the total number of pixels representing the vasculature in the thresholded image. In order to account for changes in vasculature density unrelated to branching, the total vessel length was determined. This was performed using the morphologically thinned vasculature previously mentioned. In this image, the entire vasculature is reduced to a cross-sectional width of 1 pixel. Therefore, the total number of pixels representing the vasculature is exactly equal to the total length of all vessels within the retina. To find the vessel caliber, defined as the average width of vessels, the total area of the vasculature (from the original thresholded image) was divided by the total length.

3. RESULTS

3.1 Complete knockouts have a fewer number of cells

The results obtained showed the capability of the software to determine a differing number of cells in those retinas taken from a complete knockout mouse as compared to the retinas from a partial knockout mouse. The 6-week age group images contained a mean number of cells of 108.375 for the complete knockouts and 152.875 for the partial knockouts ($p < 0.005$). Similarly, in the 3-week age group, the mean number of cells was 137 for the complete knockouts, and 177.75 for the partial knockouts ($p < 0.001$). Figure 2 shows the mean and standard deviations of the vascular cellcount within each group, along with 2 sample images to exemplify the difference between the least dense and most dense groups. As expected, the mean values are higher in the partial knockout groups than those in the complete knockout groups, supporting the fact that the *bcl-2* gene is important for survival of retinal vascular cells.

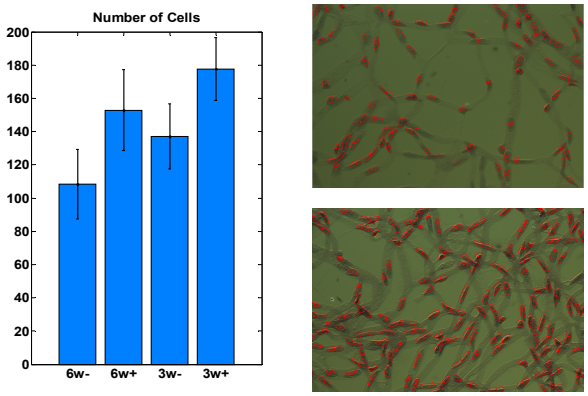

Fig. 1. Left: Mean values and Standard Deviations of cell counts of retinal vasculature over 8 fields of view. 6w is the 6 week age group, 3w is the 3 week age group. - indicates complete knockout, whereas + indicates partial knockout. Right: Sample images illustrating the difference between a low (top, 85 cells, 6w-), and a high concentration of cells (bottom, 185 cells, 3w+).

3.2 More complex retinas have higher vessel coverage

As expected, the total area of the vasculature is higher in partial knockout mice compared to the complete knockout models, and the software shows this. However, this difference is more significant at 3-weeks of age compared with 6-week-old mice. The mean values of the number of pixels representing the vasculature in the 6-week-old mice were 755250 and 869970 for complete and partial knockouts, respectively. On the other hand, the mean values within the 3-weeks old group were 763453 for complete knockouts and 862574 ($p < 0.01$) for partial knockouts. Figure 4 shows the mean and standard deviation of the vasculature area for each of the groups, along with two fields of view displaying a low and high degree of branching.

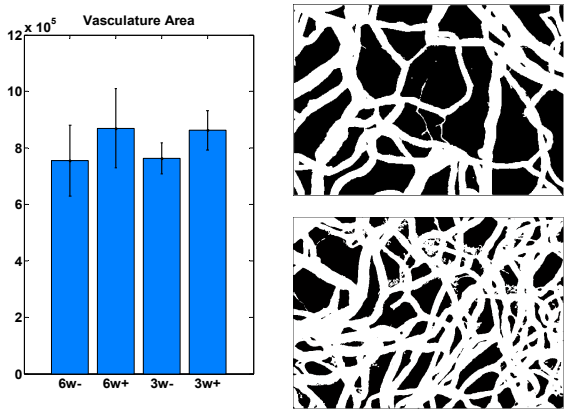

Fig. 2. Left: Mean values and Standard Deviations of cell counts of retinal vasculature over 8 fields of view. 6w is the 6 week age group, 3w is the 3 week age group. - indicates complete knockout, whereas + indicates partial knockout. Right: Sample images illustrating the difference between a small (top, 639061 pixels, 6w-), and a large area of vasculature (bottom, 954920 pixels, 3w+).

3.3 Injury model retinas have higher vessel caliber

Past studies have shown a significant correlation between the diameter of the blood vessels in the eye, termed the vessel caliber, and the level of retinopathic injury sustained in that eye[14]. For this reason, measurement of the caliber of the vessels was added to the software's capabilities. The results showed a significant difference between healthy and injured retinas in the 3 week age group, but a much smaller difference in the 6 week age group. The mean values for the vessel caliber for the complete and partial knockouts in the 6 week age group were 44.2505 and 46.4986, respectively. On the other hand, the mean values of vessel caliber for the complete and partial knockouts in the 3 week age group were 36.6427 and 45.7967 ($p < .01$), respectively. We believe the reason retinal caliber is not discriminated at the 6 week of age is related to the stage of vascular development in these mice. Retinal vasculature development consists of two phases, the first phase involves the growth of new vessels and the second phase involves the pruning and remodeling removing unnecessary vessels. A change in vessel width seems to be a precursor to a new vessel growth, and so changes in the caliber are more prominent in the growth phase of the retinal vascular development, which is seen in the early stages of growth. Therefore, we expect the vessel caliber to be a more discriminating feature at the 3 weeks of age as opposed to 6 weeks of age. Figure 3 shows the mean and standard deviations of the vessel caliber, along with sample images to illustrate fields of view with high and low caliber.

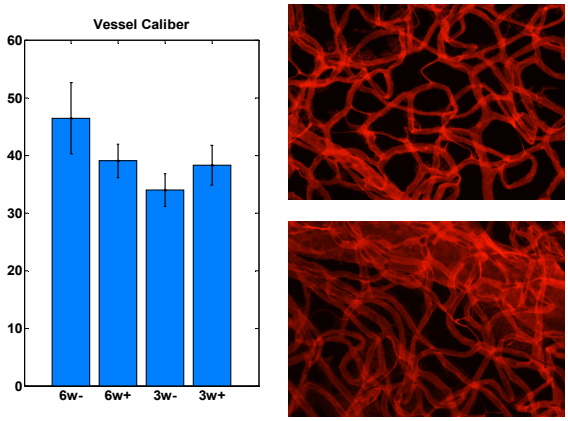

Fig. 3. Left: Mean values and Standard Deviations of Vessel Caliber of retinal vasculature over 8 fields of view. 6w is the 6 week age group, 3w is the 3 week age group. - indicates complete knockout, whereas + indicates partial knockout. Right: Sample images illustrating the difference between a small (top, 31.25 pixels, 3w-), and a thick vessel caliber (bottom,42.17 pixels, 6w+).

3.4 Classification of retinal images

With all of the aforementioned features measured, the images of the retinas were used to create a classification system in order to determine whether or not the retinas were more or less complex than their counterparts. In order to perform the classification, three classifiers were used. The first was a simple linear classifier, which looks for a linear plane to separate the classes[15]. The second classifier used was a support vector machine, which attempts to maximize the margin for error in classification[16]. This classifier used radial basis functions and the kernel trick to project the data into a high dimensional space for easier separation. In addition, the cost was kept at a relatively low value to allow for better generalization of the results. Finally, a k-nearest-neighbors classifier was used on the data points, which classifies each point depending on the majority of its neighbors[17]. For this system, the number of neighbors used to determine the classification was 4. A majority vote was then taken between these three classifiers to determine the class of an image. In the event of a tie, k-nearest-neighbors was given the highest priority, followed by the support vector machine, and lastly the linear classifier.

Figure 4 shows the distribution of two of the features used in classification between the four groups. In both the 3 and 6 week age group, classification accuracy was 81.25%. In addition, when classifying for gene presence regardless of age, accuracy was 81.25%. These accuracies were determined using the leave-one-out method. In this method, one data point is withheld, the system is trained using all of the other data points available, and the withheld data point is then classified into one of the groups. This process is then repeated for every data point available, and the error rate is the number of data points that were not correctly classified into their original group.

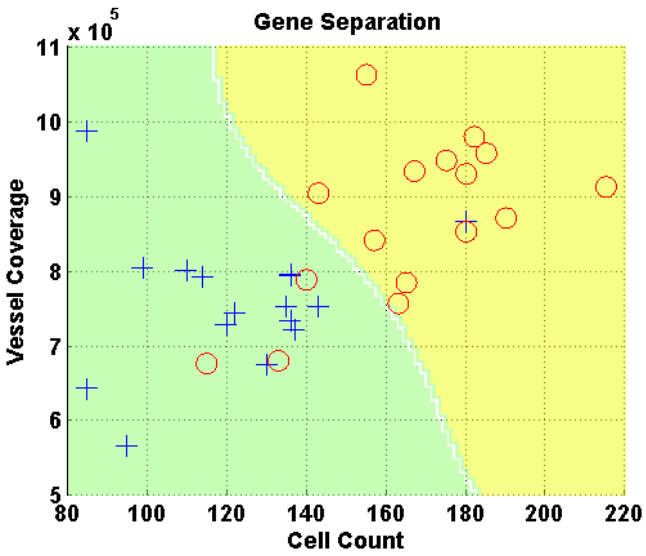

Fig. 4. Visualization of the separation of the partial and complete knockouts using two of the features extracted from each image. Blue crosses represent complete knockouts, whereas red circles indicate only partial knockouts. Green and yellow regions represent different decisions. Data shown is from both age groups (3 weeks and 6 weeks).

4. DISCUSSION

We have created a system capable of classifying retinal vasculature images based on their complexity. This software is capable of automated detection of various features corresponding to the vasculature in the retina. This task has traditionally been performed manually, a process which is both tedious and prone to error. The automation of these tasks will lead to a more reliable and robust measurement. The features used for this classification include the cell count, vessel coverage, and vessel caliber. The cell count is an important indicator of retinopathy, as it is directly related to loss of existing or the growth of new vessels, specifically due to the change in the density of pericytes and endothelial cells[4, 18]. Therefore, we expect the changes in the density of the vascular cells in the retina to be a precursor to retinopathic injury. Evidence of the difference between a healthy and injured eye can be seen in Figure 1. The second feature measured from each image was the total vasculature coverage in the retina. This is an important feature, as more complex retinas will assuredly be more dense in each field of view, leading to a higher total for the area of the vasculature. The results in Figure 2 show these results hold true for the data studied here. The third feature measured in this study was the vessel caliber, i.e. the average width of a blood vessel in each field of view. Previous studies have shown a correlation between the vessel caliber and the degree of retinopathy present in a retina, indicating that an increase in caliber may be a precursor to retinopathic injury[11]. Figure 3 shows the results obtained from our study, where the complete knockout retinas had a smaller caliber as compared to their partial knockout counterparts. Finally, classification can be performed using the measured features to determine a retina's health status. Figure 4 shows the separation of healthy and injured retinas in terms of two of the extracted features. With further development, this software system will aid in the development of cellular level detection methodology for the evaluation of retinopathic changes in a non-invasive manner when imaged *in vivo*.

ACKNOWLEDGEMENT

We would like to acknowledge the support of UWM research fellow award. CMS was funded, in part, by DK067120 from the National Institutes of Health and AHA research award (0950057G). NS is supported by NIH grants EY016995, and RC4 EY 021357 (NS) and an unrestricted departmental award from Research to Prevent Blindness. NS is a recipient of a Research Award from American Diabetes Association (1-10-BS-160) and Retina Research Foundation.

REFERENCES

[1] Klein, R., Klein, B. E., Moss, S. E., Davis, M. D., and DeMets, D. L., "The Wisconsin epidemiologic study of diabetic retinopathy. II. Prevalence and risk of diabetic retinopathy when age at diagnosis is less than 30 years," Arch Ophthalmol 102(4), 520-6 (1984).

[2] Wong, T. Y., and Mitchell, P., "Hypertensive retinopathy," N Engl J Med 351(22), 2310-7 (2004).

[3] Bressler, N. M., Bressler, S. B., and Fine, S. L., "Age-related macular degeneration," Survey of Ophthalmology 32(6), 375-413 (1988).

[4] Hammes, H. P., Lin, J., Renner, O., Shani, M., Lundqvist, A., Betsholtz, C., Brownlee, M., and Deutsch, U., "Pericytes and the pathogenesis of diabetic retinopathy," Diabetes 51(10), 3107-12 (2002).

[5] Sjolie, A. K., Stephenson, J., Aldington, S., Kohner, E., Janka, H., Stevens, L., and Fuller, J., "Retinopathy and vision loss in insulin-dependent diabetes in Europe. The EURODIAB IDDM Complications Study," Ophthalmology 104(2), 252-60 (1997).

[6] Field, M. G., Elner, V. M., Puro, D. G., Feuerman, J. M., Musch, D. C., Pop-Busui, R., Hackel, R., Heckenlively, J. R., and Petty, H. R., "Rapid, noninvasive detection of diabetes-induced retinal metabolic stress," Arch Ophthalmol 126(7), 934-8 (2008).

[7] White, M. C., Kohner, E. M., Pickup, J. C., and Keen, H., "Reversal of diabetic retinopathy by continuous subcutaneous insulin infusion: a case report," Br J Ophthalmol 65(5), 307-11 (1981).

[8] Tapp, R. J., Shaw, J. E., Harper, C. A., de Courten, M. P., Balkau, B., McCarty, D. J., Taylor, H. R., Welborn, T. A., Zimmet, P. Z., and Grp, A. S., "The prevalence of and factors associated with diabetic retinopathy in the Australian population," Diabetes Care 26(6), 1731-1737 (2003).

[9] Joussen, A. M., Murata, T., Tsujikawa, A., Kirchhof, B., Bursell, S. E., and Adamis, A. P., "Leukocyte-mediated endothelial cell injury and death in the diabetic retina," Am J Pathol 158(1), 147-52 (2001).

[10] Huang, Q., Wang, S., Sorenson, C. M., and Sheibani, N., "PEDF-deficient mice exhibit an enhanced rate of retinal vascular expansion and are more sensitive to hyperoxia-mediated vessel obliteration," Exp Eye Res 87(3), 226-41 (2008).

[11] Klein, R., Klein, B. E., Moss, S. E., Wong, T. Y., Hubbard, L., Cruickshanks, K. J., and Palta, M., "The relation of retinal vessel caliber to the incidence and progression of diabetic retinopathy: XIX: the Wisconsin Epidemiologic Study of Diabetic Retinopathy," Arch Ophthalmol 122(1), 76-83 (2004).

[12] Smith, L. E., Kopchick, J. J., Chen, W., Knapp, J., Kinose, F., Daley, D., Foley, E., Smith, R. G., and Schaeffer, J. M., "Essential role of growth hormone in ischemia-induced retinal neovascularization," Science 276(5319), 1706-9 (1997).

[13] Wang, S. J., Sorenson, C. M., and Sheibani, N., "Attenuation of retinal vascular development and neovascularization during oxygen-induced ischemic retinopathy in Bcl-2-/- mice," Developmental Biology 279(1), 205-219 (2005).

[14] Klein, R., Klein, B. E. K., Moss, S. E., Wong, T. Y., Hubbard, L., Cruickshanks, K. J., and Palta, M., "The relation of retinal vessel caliber to the incidence and progression of diabetic retinopathy - XIX: The Wisconsin epidemiologic study of diabetic retinopathy," Archives of Ophthalmology 122(1), 76-83 (2004).

[15] Fan, R. E., Chang, K. W., Hsieh, C. J., Wang, X. R., and Lin, C. J., "LIBLINEAR: A Library for Large Linear Classification," Journal of Machine Learning Research 9, 1871-1874 (2008).

[16] Cortes, C., and Vapnik, V., "Support-Vector Networks," Machine Learning 20(3), 273-297 (1995).

[17] Cover, T., Hart, P., "Nearest neighbor pattern classification," IEEE Transactions on Information Theory 13(1), 21-27 (1967).

[18] Armulik, A., Abramsson, A., and Betsholtz, C., "Endothelial/pericyte interactions," Circ Res 97(6), 512-23 (2005).

[19] Spranger, J., and Pfeiffer, A. F. H., "New concepts in pathogenesis and treatment of diabetic retinopathy," Experimental and Clinical Endocrinology & Diabetes 109, S438-S450 (2001).